Available online at www.sciencedirect.com
ScienceDirect
Applied Catalysis B: Environmental 78 (2008) 381–387
APPLIED CATALYSIS B: ENVIRONMENTAL
www.elsevier.com/locate/apcatb

Direct alcohol fuel cells: A novel non-platinum and alcohol inert ORR electrocatalyst

Shuqin Song [a,*], Yi Wang [a], Panagiotis Tsiakaras [b], Pei Kang Shen [a]

[a] State Key Laboratory of Optoelectronic Materials and Technologies, School of Physics and Engineering, Sun Yat-Sen University, Guangzhou 510275, China
[b] Department of Mechanical Engineering, School of Engineering, University of Thessaly, Pedion Areos 383 34, Greece

Received 6 June 2007; received in revised form 18 September 2007; accepted 21 September 2007
Available online 3 October 2007

Abstract

In the present investigation, a series of binary Pd_xFe_y/C electrocatalysts for the oxygen reduction reaction (ORR) was synthesized in a very short time by employing a pulse-microwave assisted polyol method. The physico-chemical properties were obtained by employing the techniques of X-ray diffraction (XRD) and transmission electron microscopy (TEM). The electrochemical activity was studied by the aid of the techniques of cyclic voltammetry and rotating disk electrode. Based on the obtained experimental results, it can be deduced that the addition of Fe increases the activity of Pd towards the reaction of oxygen reduction. More precisely, when the molar ratio between Pd and Fe was 3:1, the highest oxygen reduction activity among all the investigated Pd_xFe_y/C catalysts was obtained. It was also found that Pd_3Fe_1/C exhibited an oxygen reduction activity comparable to that of Pt/C, while showed almost no activity for alcohols oxidation. Moreover, in the simultaneous presence of both methanol and oxygen, Pd_3Fe_1/C displayed an excellent selectivity for oxygen reduction reaction.

Keywords: Oxygen reduction reaction (ORR); Pd_xFe_y/C electrocatalysts; Direct alcohol fuel cells (DAFCs); Alcohol crossover

1. Introduction

Alcohol crossover is one of the main barriers hindering the wide application and commercialization of direct alcohol fuel cells (DAFCs) due to the fact that the present commonly used Pt-based cathode catalysts are also active to alcohols oxidation [1,2]. This consequently leads to a mixed potential at the cathode through the short chemical reaction, decreasing in this way the cathode performance [3]. At the same time, alcohol crossover results in lower fuel utilization efficiency and increases the difficulty in the water, fuel and thermal management of the system. Except for the attempts to search for novel electrolytes resistant to alcohols [4–6], an alternative and most effective means of overcoming the above difficulties is to identify non-platinum based cathode electrocatalysts with high activity to oxygen reduction reaction (ORR), and at the same time with tolerance to alcohol oxidation.

Besides the excellent tolerance to alcohol, the cathode catalysts should possess the desirable ORR activity because its corresponding overpotential in PEMFCs is about 0.2 V even under open circuit conditions, due to the highly irreversible process of oxygen reduction reaction [7]. In the volcano plot of oxygen reduction *versus* d-orbital vacancies [8], Pd exhibits a similar activity to oxygen reduction with respect to Pt. However, Pd-based cathode catalysts may be more appropriate for DAFCs, because Pd is insensitive for the adsorption and oxidation of alcohol [9–10]. Moreover, the mineable resources of palladium are larger than that of platinum. Although the corrosion stability of Pd is inferior to that of Pt, recently, it was reported that binary and ternary Pd-based alloys such as PdCo [11–15], PdFe [10,16], Pd–Co–Au and Pd–Co–Mo [15] displayed a comparable activity and higher selectivity to oxygen reduction reaction. In the present investigation, a series of Pd_xFe_y/C with different Pd/Fe feed weight molar ratio were prepared by a pulse microwave assisted polyol synthesis method in a very short time (2 min). Their corresponding physico-chemical characteristics were obtained by using the techniques of X-ray diffraction (XRD) and transmission

* Corresponding author. Tel.: +86 20 84113369; fax: +86 20 84113369.
E-mail address: stsssq@mail.sysu.edu.cn (S. Song).

0926-3373/$ – see front matter © 2007 Elsevier B.V. All rights reserved.
doi:10.1016/j.apcatb.2007.09.037

electron microscopy (TEM). The ORR activity and the tolerance to alcohol oxidation were evaluated by employing the electrochemical methods of cyclic voltammetry (CV) and rotating disk electrode (RDE), in acidic environment in the absence or presence of alcohol.

2. Experimental

2.1. Catalyst preparation

The 20 wt. % Pd_xFe_y/C (x and y denotes the molar ratio for Pd and Fe, respectively) electrocatalysts were fast and easily prepared by a pulse-microwave assisted polyol synthesis method [17]. The primary steps of this synthesis process are given as follows: In a beaker, the starting precursors ($PdCl_2$ and $FeCl_3$) were well mixed with ethylene glycol (EG) in an ultrasonic bath, and then XC-72 R carbon black (Cabot Corp., S_{BET} = 236.8 $m^2\ g^{-1}$) was added into the mixture. After the pH value of the system was adjusted to be 13 by the drop-wise addition of 1.0 mol L^{-1} NaOH/EG, a well-dispersed slurry was obtained with ultrasonic stirring for 30 min. Thereafter, the slurry was microwave-heated in the pulse form with every 5 s for several times. In order to promote the adsorption of the suspended metal nanoparticles onto the support, hydrochloric acid was adopted as the sedimentation promoter and the solution was re-acidified with a pH value of about 5. The resulting black solid sample was filtered, washed and dried at 80 °C for 10 h in a vacuum oven. For the sake of comparison, 20 wt.% Pt/C was also prepared and examined in the same way.

2.2. Catalyst characterization

The XRD measurements were carried out on a D/Max-IIIA (Rigaku Co., Japan) using Cu K_α radiation (λ = 0.15406 nm), and operating at 40 kV and 40 mA. The 2θ angular regions between 10 and 90° were explored at a scan rate of 5° min^{-1}. The TEM images of the samples were obtained by using the JEOL JEM-2010 (HR) electron microscope operated at 200 kV.

All electrochemical measurements were conducted on a PARSTAT 2273 instrument, in a standard three-electrode cell at room temperature, adopting a saturated calomel electrode (SCE) and a platinum foil as the reference electrode and the counter electrode, respectively. A glass carbon (GC) disk electrode, polished to a mirror-finish with a 0.05 μm alumina suspension before each experiment, was used as substrate for the electrocatalyst thin film in the electrochemical measurements. The thin film catalyst layer as the working electrode was prepared as follows: a mixture containing 5.0 mg electrocatalyst, 0.9 mL ethanol and 0.1 mL Nafion solution (5 wt.%) was stirred ultrasonically for 15 min to obtain a well-dispersed ink. The geometric area of the electrode was 0.1963 cm^2. The catalyst ink was then quantitatively transferred onto the surface of the glass carbon electrode by using a micropipette, and dried under infrared lamp to obtain a catalyst thin film. An aqueous solution containing 0.5 mol L^{-1} H_2SO_4 in the absence or in the presence of 0.5 mol L^{-1} alcohols was used as the electrolyte, which was deareated with high-purity nitrogen gas during the characterization by cyclic voltammetry. The scanning potential was ranging from −0.2415 to 1.0 V (*vs.* SCE) at a sweeping rate of 20 mV s^{-1}. For the ORR experiment, the electrolyte was saturated with oxygen, with a potential range from 0.9 to 0 V (*vs.* SCE) and a scan rate of 5 mV s^{-1}. It should be noted that all the potential is referred to SCE without specification.

3. Results and discussion

XRD patterns for the as-prepared Pd_xFe_y/C catalyst are shown in Fig. 1. As shown, all the Pd_xFe_y/C catalysts present a typical fcc pattern, with diffraction angles shifting to a little higher positions with respect to those of Pd. This gives an indicator that the lattice of Pd was contracted due to its part displacement by Fe. There are no Fe^0 or iron oxides diffraction peaks observed in the XRD patterns of all the examined Pd_xFe_y/C electrocatalysts. This could be probably due to the fact that their phases were not fully developed or their particles sizes were smaller than the detection limit of the XRD. Table 1 lists the particle sizes and the corresponding lattice parameters calculated from the Pd (2 2 0) diffraction line using the Scherrer formula and Bragg equations, respectively [18]. It can be clearly seen from Table 1 that the lattice parameter decreases in the order: Pd/C > Pd_1Fe_1/C ≈ Pd_2Fe_1/C > Pd_4Fe_1/C > Pd_3Fe_1/C. Although in the present case the samples were not thermally treated, the same results as those reported in literature were recorded [10].

The TEM images of Pd_xFe_y/C (here only for the Pd_3Fe_1/C sample) and Pt/C are given in Fig. 2 (A) and (B), respectively. It can be clearly seen that Pd_3Fe_1/C is characterized by a much bigger particle size and poor distribution compared with Pt/C. However, Pd_3Fe_1/C still exhibits a comparable performance for ORR to Pt/C, besides its interesting tolerance to alcohol oxidation, which will be discussed in the following part. This suggests that a further decrease in the particle size of Pd_3Fe_1/C will result in a promising increase of its corresponding activity towards ORR.

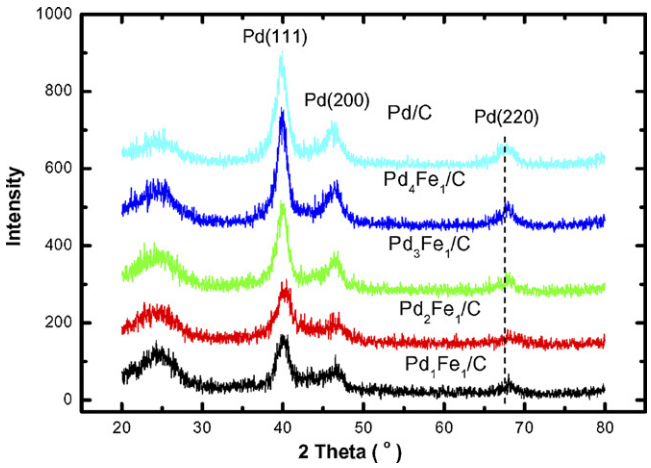

Fig. 1. XRD results of the as-prepared carbon supported Pd_xFe_y/C based electrocatalysts.

Table 1
Structural parameters of the as-prepared Pd_xFe_y/C catalysts

Samples	Particle size (nm)	Lattice parameter (nm)
Pd/C	3.8	0.3910
Pd_4Fe_1/C	4.3	0.3894
Pd_3Fe_1/C	2.8	0.3886
Pd_2Fe_1/C	3.4	0.3900
Pd_1Fe_1/C	4.4	0.3902

Fig. 3(A) shows the ORR polarization curves for all the Pd_xFe_y/C catalysts in oxygen saturated 0.5 mol L^{-1} H_2SO_4 solution obtained by using a rotating disk electrode at 2500 rpm and at a scanning rate of 5 mV s^{-1}. It can be distinguished that the introduction of Fe into Pd can increase Pd's activity towards oxygen reduction reaction. For the further analysis of the relationship between the enhanced activity of Pd_xFe_y/C catalysts and their structural characteristics, the corresponding

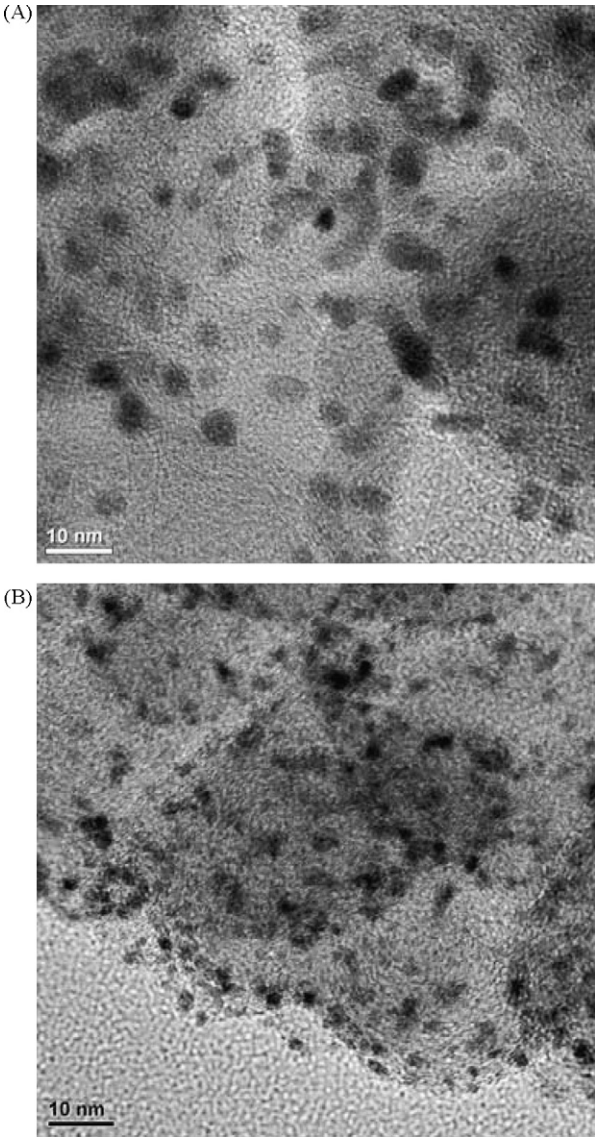

Fig. 2. TEM images of the as-prepared Pd_3Fe_1/C (A) and Pt/C (B).

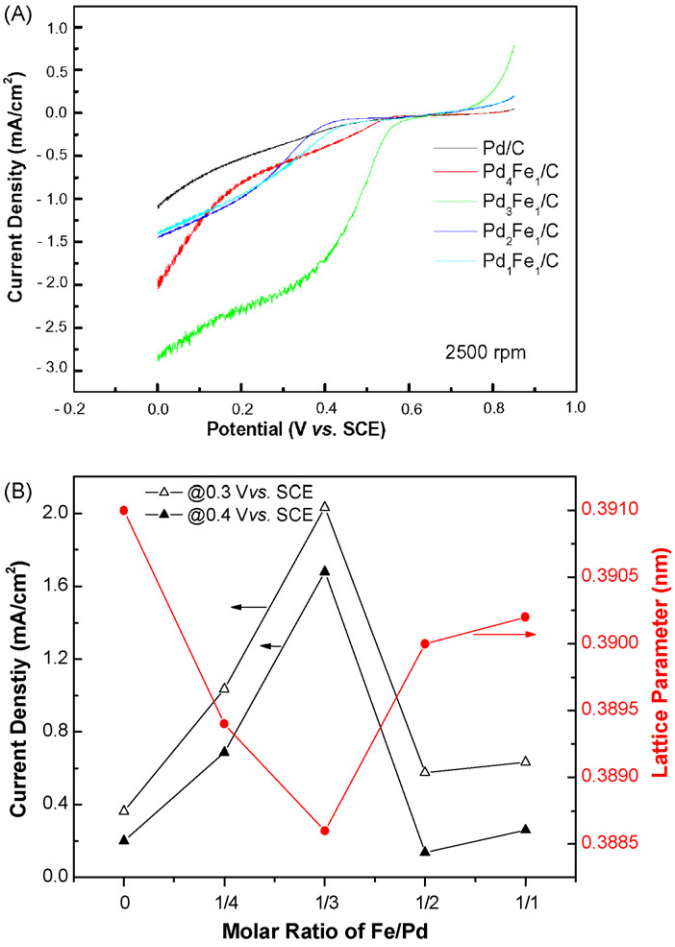

Fig. 3. (A) Polarization curves for the oxygen reduction reaction over Pd_xFe_y/C series electrocatalysts in oxygen saturated 0.5 mol L^{-1} H_2SO_4. (B) The corresponding current density at 0.3 and 0.4 V (*vs.* SCE) over Pd-based series catalyst and the lattice parameters of Pd calculated from XRD data against the molar ratio of Fe/Pd in Pd_xFe_y/C electrocatalysts; metal loading = 0.127 mg cm^{-2}; rotation rate: 2500 rpm; sweeping rate: 5 mV s^{-1}.

current density at 0.3 and 0.4 V (*vs.* SCE) over Pd-based series catalyst and the lattice parameters of Pd calculated from XRD data against the molar ratio of Pd/Fe in the Pd_xFe_y/C electrocatalysts were plotted as shown in Fig. 3(B). It can be clearly seen that a volcano-type relationship between the Pd/Fe molar ratio and their corresponding ORR activity exists. When the molar ratio between Pd and Fe was 3:1, the best oxygen reduction activity behavior was obtained. It can also be seen from Fig. 3(B) that, in the case of Pd_3Fe_1/C, Pd–Pd bond contracts to the most degree, which probably contributes to its desirable performance for oxygen reduction reaction. This is similar to the case of Pt–M alloys, where the peak in activity was found for an optimal Pt–Pt bond [19].

For the further evaluation of the Pd_3Fe_1/C activity towards oxygen reduction reaction, the ORR polarization curves over Pt/C and Pd_3Fe_1/C were carried out and compared in oxygen saturated 0.5 mol L^{-1} H_2SO_4 aqueous solution at a sweeping rate of 5 mV s^{-1}. These results are shown in Fig. 4. As it can be distinguished, the electrocatalytic current increases along with the rotation rate increment. The higher currents at higher rotation rates correspond to a higher catalyst turnover rate for

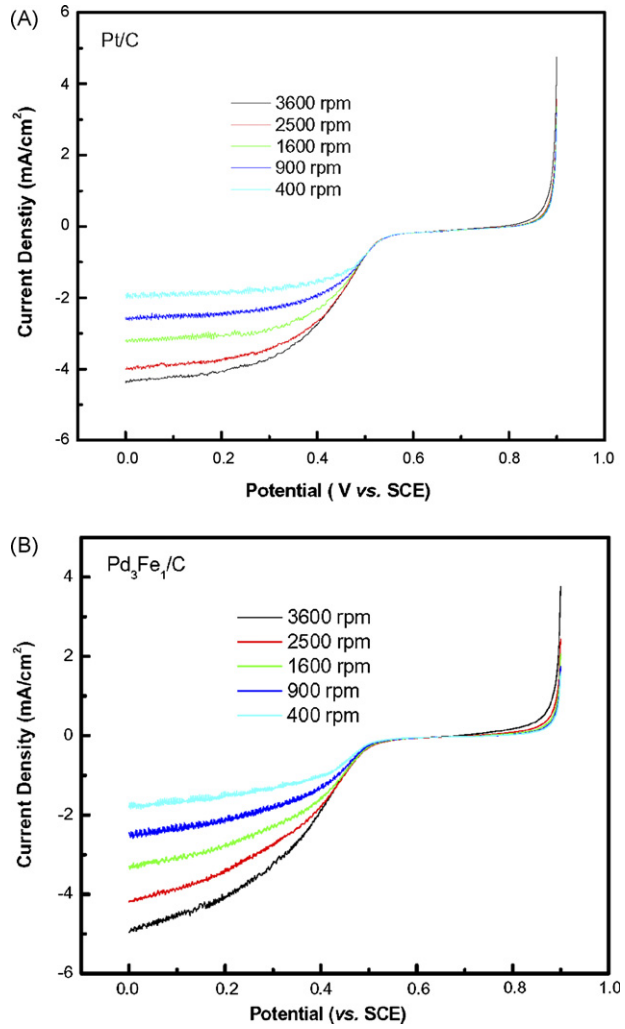

Fig. 4. Polarization curves for the oxygen reduction reaction over (A) Pt/C and (B) Pd_3Fe_1/C in oxygen saturated 0.5 mol L^{-1} H_2SO_4 at different rotating rates. Sweeping rate: 5 mV s^{-1}.

oxygen reduction reaction on the electrode. By comparing the ORR activity over Pt/C and Pd_3Fe_1/C, it can be clearly seen that at any rotation rate they both exhibit a comparable performance, which is in agreement with the already reported results [10]. The Pd_3Fe_1/C activity towards ORR could be attributed to the decreased inter-atomic spacing, the increased Pd 5d-orbital vacancies and a possible direct role of the surface atoms of Fe. This direct role has been suggested to be through interactions with oxygen species or through activity as a redox mediator [20]. Lambrou et al. found that in a Pd–Rh/CeO_2–Al_2O_3 three way catalyst, iron acts as an oxygen storage component under oxidizing conditions through the process $Fe \rightarrow FeO \rightarrow Fe_3O_4 \rightarrow (FeO{\cdot}Fe_2O_3) \rightarrow Fe_2O_3$ [21]. In the present case, Fe might also act as a redox mediator. The contribution of Fe to the desired ORR performance of Pd_3Fe_1/C could also be explained as follows: it is well known that Fe is an electropositive element, to which the oxygen species are easily attached, providing an electrostatic force that mainly favors four-electron oxygen reduction pathways, improving consequently the catalyst's ORR activity [22–24]. As known, oxygen reduction reaction mainly takes place according to the following two pathways in acidic environment [25].

Direct four-electron pathway :

$$O_2 + 4H^+ + 4e^- \rightarrow 2H_2O \quad (1)$$

Two-electron pathway : $O_2 + 2H^+ + 2e^- \rightarrow H_2O_2$ (2)

with the following further reactions:

$$H_2O_2 + 2H^+ + 2e^- \rightarrow 2H_2O \quad (3a)$$

or

$$2H_2O_2 \rightarrow 2H_2O + O_2 \quad (3b)$$

The kinetic process for catalytic oxygen reduction reaction on the thin film electrode can be analyzed by a Koutecký-Levich plot. Fig. 5 displays the corresponding Koutecký-Levich plot for ORR at a potential of 0.1 V (*vs.* SCE) on the RDE coated with Pt/C or Pd_3Fe_1/C in O_2 saturated 0.5 mol L^{-1} H_2SO_4 aqueous solution. It is obvious that in the case of Pd_3Fe_1/C, the line has a higher slope than that over Pt/C. From the following equation [26], the slope ($1/B$) is directly related to the total number of electrons (n) involved in oxygen reduction:

$$\frac{1}{I} = \frac{1}{I_k} + \frac{1}{B(\omega)^{1/2}} \quad (4)$$

where I is the experimentally observed current, I_k is the kinetic current, B is equal to $0.62nFAC_{O_2}(D_{O_2})^{2/3}\nu^{-1/6}$, ω is the rotation rate in rad s^{-1}, F is the Faraday constant, A is the electrode area, C_{O_2} is the bulk concentration of O_2, D_{O_2} is the diffusion coefficient for O_2 and ν is the kinematic viscosity of the electrolyte. From the reported results [26], it is known that oxygen reduction reaction over Pt passes through the four-electron pathway as discussed above. As a result, the higher slope in Pd_3Fe_1/C case could be attributed to the fact that the oxygen reduction reaction proceeds not only through the four-electron pathway, but also through the peroxide (two-electron) pathway. The latter is supported from the literature [27] where it has been reported that Pd can act as the cathode catalyst to *in*

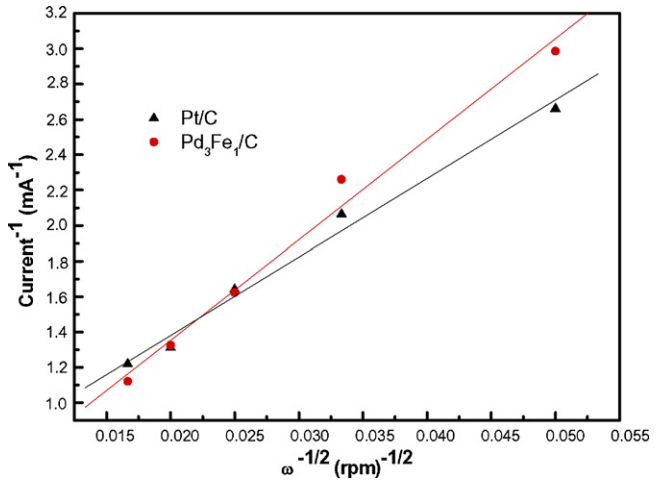

Fig. 5. Koutechý-Levich plots for oxygen reduction at 0.1 V (*vs.* SCE) at Pt/C and Pd_3Fe_1/C, respectively, in O_2 saturated 0.5 mol L^{-1} H_2SO_4 solution.

situ generate H_2O_2 for phenol and electricity cogeneration at lower potential. This suggests that over Pd catalysts most probably the oxygen reduction reaction takes place following mainly the peroxide (two-electron) pathway at lower potential. Even in this case, from Fig. 5 it can be seen that Pd_3Fe_1/C still exhibits comparable ORR activity to Pt, which could be due to kinetic reasons and especially to higher kinetic constant values. This appears clearly in Fig. 5, from the decreased intercept compared to that of Pt/C.

For the cathode electrocatalysts of direct alcohol fuel cells, except for its desirable ORR activity, another interesting property is the tolerance to alcohol oxidations. Cyclic voltammetry was adopted to check whether or not Pd_3Fe_1/C is active to alcohol oxidation in 0.5 mol L^{-1} H_2SO_4 aqueous solutions in the absence or presence of 0.5 mol L^{-1} CH_3OH (or C_2H_5OH) at room temperature. One can distinguish from Fig. 6(A) that in the case of Pt/C, the presence of alcohol obviously obscured the hydrogen adsorption and desorption. Moreover, methanol (ethanol) starts to be oxidized at the potential of about 0.3 V (0.5 V) (*vs.* SCE). Despite the fact that in the case of Pd_3Fe_1/C, as shown in Fig. 6(B), the existence of methanol or ethanol can also affect the hydrogen adsorption and desorption, this effect is quite small compared with that over Pt/C. On the other hand, it can be distinguished from Fig. 6(B) that methanol and ethanol cannot be oxidized over Pd_3Fe_1/C at all. By comparing these two cases, one can observe that the alcohol oxidation current density on Pd_3Fe_1/C is negligible compared with that on the Pt/C catalyst. This suggests that this catalyst possesses excellent tolerance to alcohol oxidation compared with Pt/C, which enables its potential application in direct alcohol fuel cells.

In the present work the selectivity of Pd_3Fe_1/C and Pt/C to ORR in the simultaneous presence of methanol and oxygen were also investigated and compared, and the results are displayed in Fig. 7. In the presence of 0.5 mol L^{-1} CH_3OH, over Pt/C, methanol starts oxidizing at *ca.* 630 mV and reaches peak values at about 440 mV as shown in Fig. 7(A). Then, the combined results of methanol oxidation and oxygen reduction lead to a slightly rising limiting current density, which is lower than that obtained in 0.5 mol L^{-1} H_2SO_4 in the absence of methanol. This indicates that in the fuel cell operation mode, when Pt/C is adopted as the cathode catalyst, the permeated methanol from the anode will consequently lead to a decreased

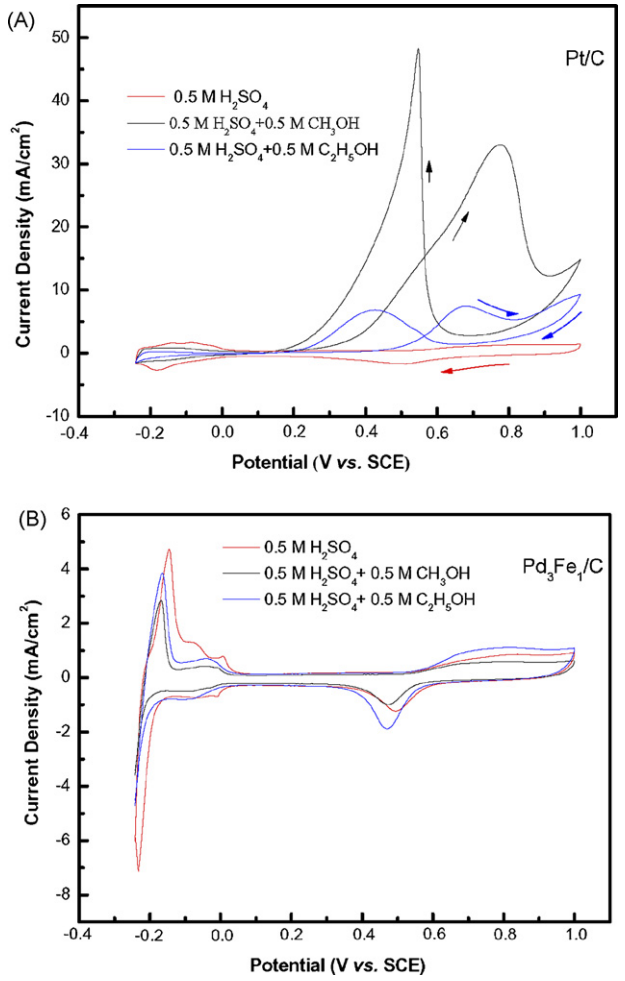

Fig. 6. Cyclic voltammograms of Pt/C (A) and Pd_3Fe_1/C (B) in N_2 -saturated 0.5 mol L^{-1} H_2SO_4 aqueous solutions in the absence or presence of 0.5 mol L^{-1} CH_3OH or 0.5 mol L^{-1} C_2H_5OH. Sweep rate = 20 mV s^{-1}; metal loading = 0.127 mg cm^{-2}.

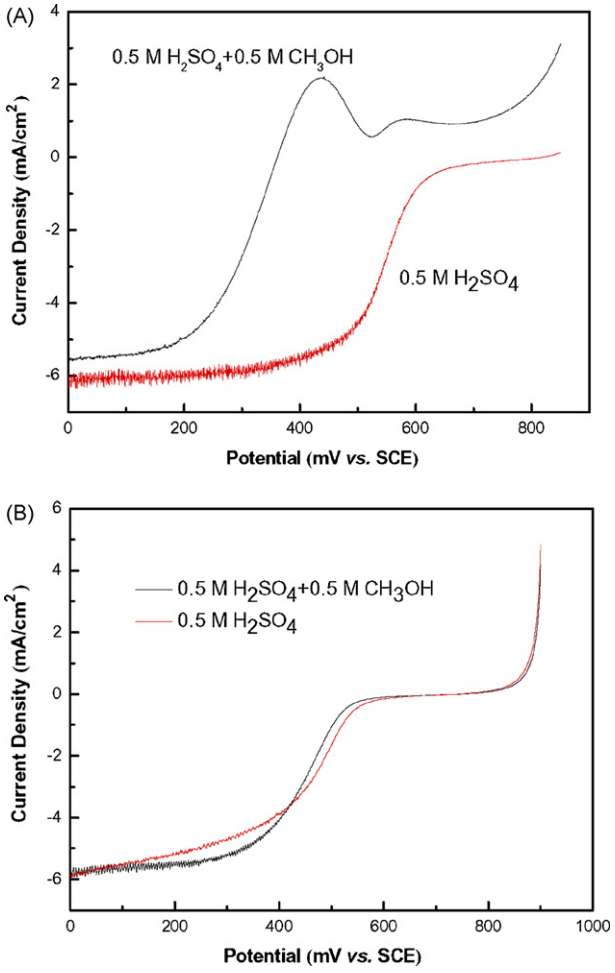

Fig. 7. Polarization curves for the oxygen reduction reaction over Pt/C (A) and Pd_3Fe_1/C (B) in oxygen saturated 0.5 mol L^{-1} H_2SO_4 with or without 0.5 mol L^{-1} CH_3OH. Rotation rates: 2500 rpm; sweep rate: 5 mV s^{-1}; room temperature.

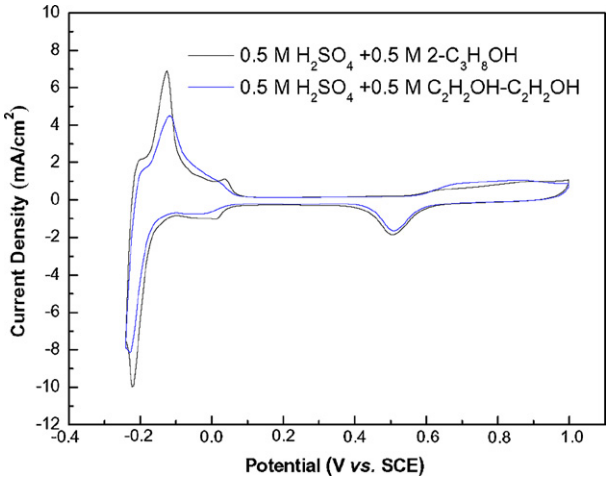

Fig. 8. Cyclic voltammograms of Pd_3Fe_1/C in N_2-saturated 0.5 mol L^{-1} H_2SO_4 aqueous solutions with 2-propanol and ethylene glycol with a concentration of 0.5 mol L^{-1}. Sweep rate = 20 mV s^{-1}; metal loading = 0.127 mg cm^{-2}.

cell performance resulting from the mixed potential formed at the cathode [3]. However, under the same operating conditions, in the case of Pd_3Fe_1/C, the addition of methanol to 0.5 mol L^{-1} H_2SO_4 solution has almost no effect on the ORR activity as seen from Fig. 7(B). This suggests that Pd_3Fe_1/C possesses an excellent selectivity to ORR in the presence of both methanol and oxygen simultaneously. As described above, the as-prepared Pd_3Fe_1/C not only exhibits a comparable performance for ORR with respect to Pt/C, but also displays an excellent tolerance to methanol oxidation, which is quite interesting and attractive for the cathode catalyst of direct alcohol fuel cells. Kinoshita also reported that platinum and palladium showed the similar behavior to ORR [28], while they possessed quite different characteristics for methanol oxidation. The former is of high activity, while the latter is completely inactive to methanol oxidation in acid solutions [29].

In order to check the tolerance of the as-prepared Pd_3Fe_1/C to the fuel candidates for direct alcohol fuel cells, the cyclic voltammetry was also recorded in 0.5 mol L^{-1} H_2SO_4 aqueous solutions containing 2-propanol and glycol with a concentration of 0.5 mol L^{-1}, respectively. The corresponding CV curves are given in Fig. 8. It can be distinguished from Fig. 8 that Pd_3Fe_1/C has no any activity to 2-propanol and glycol oxidation either, with the same behavior as methanol and ethanol. This suggests that Pd_3Fe_1/C has a potential application in direct alcohol fuel cells. That is due to the fact that Nafion® membranes are still the commonly adopted electrolyte for DAFCs, through which alcohol crossover cannot be avoided due to the similar molecular structure of alcohol and water.

4. Conclusions

In the present investigation, novel Pd_xFe_y/C electrocatalysts for oxygen reduction reaction were synthesized by a pulse microwave assisted polyol technique and characterized by the XRD, TEM, CV and RDE techniques. Based on the experimental results, it could be concluded that the use of the combined pulse microwave technique and modified polyol synthesis method is an effective way to get nano carbon supported electrocatalysts with high dispersion in a very short time. From the electrochemical results, it can be concluded that the addition of Fe can increase the activity of Pd towards oxygen reduction reaction. When the molar ration between Pd and Fe was 3:1, Pd_xFe_y/C exhibited a comparable activity for ORR with respect to Pt/C. From the joint results of CV and RDE, it can be concluded that Pd_3Fe_1/C displayed also an excellent tolerance to alcohol electro-oxidation. Moreover, in the presence of both alcohol and oxygen, Pd_3Fe_1/C possessed high selectivity to oxygen reduction reaction. From these results, it is suggested that Pd_3Fe_1/C is a potential promising cathode electrocatalyst for direct alcohol fuel cells.

Acknowledgements

The authors gratefully acknowledge the financial support from ‘‘the Scientific Research Foundation for Young Teachers of the Sun Yat-Sen University’’ and ‘‘Guangdong Province Industrial Key Technology R&D Program (2006A10704001)’’.

References

[1] S. Song, P. Tsiakaras, Appl. Catal. B 63 (2006) 187–193.
[2] S. Song, W. Zhou, Z. Liang, R. Cai, G. Sun, Q. Xin, V. Stergiopoulos, P. Tsiakaras, Appl. Catal. B 55 (2005) 65–72.
[3] H. Uchida, Y. Mizuno, M. Watanabe, Chem. Lett. (2000) 1268–1269.
[4] Y. Fu, A. Manthiram, M.D. Guiver, Electrochem. Commun. 9 (2007) 905–910.
[5] V.K. Shahi, Solid State Ionics 177 (2007) 3395–3404.
[6] S. Zhong, X. Cui, H. Cai, T. Fu, C. Zhao, H. Na, J. Power Sources 164 (2007) 65–72.
[7] A.S. Arico, S. Srinivasan, V. Antonucci, Fuel Cells 1 (2001) 133–161.
[8] S. Mukerjee, S. Srinivasan, M.P. Soriaga, J. Electrochem. Soc. 142 (1995) 1409–1422.
[9] O. Savadogo, K. Lee, K. Oishi, S. Mitsushima, N. Kamiya, K.I. Ota, Electrochem. Commun. 6 (2004) 105–109.
[10] M.H. Shao, K. Sasaki, R.R. Adzic, J. Am. Chem. Soc. 128 (2006) 3526–3527.
[11] W. Wang, D. Zheng, C. Du, Z. Zou, J. Power Sources 167 (2007) 243–249.
[12] J.L. Fernandez, D.A. Walsh, A.J. Bard, J. Am. Chem. Soc. 127 (2005) 357–365.
[13] J.L. Fernandez, V. Raghuveer, A. Manthiram, A.J. Bard, J. Am. Chem. Soc. 127 (2005) 13100–13101.
[14] V. Raghuveer, A. Manthiram, A.J. Bard, J. Phys. Chem. B 109 (2005) 22909–22912.
[15] V. Raghuveer, P.J. Ferreira, A. Manthiram, Electrochem. Commun. 8 (2006) 807–814.
[16] M.R. Tarasevich, G.V. Zhutaeva, V.A. Bogdanovskaya, M.V. Radina, M.R. Ehrenburg, A.E. Chalykh, Electrochim. Acta 52 (2007) 5108–5118.
[17] S. Song, Y. Wang, P. Shen, J. Power Sources 170 (2007) 46–49.
[18] V. Radmilovic, H.A. Gasteiger, P.N. Ross, J. Catal. 154 (1995) 98–106.
[19] S. Mukerjee, S. Srinivasan, M.P. Soriage, J. McBreen, J. Electrochem. Soc. 142 (1995) 1409–1422.
[20] W. Vielstich, A. Lamm, H.A. Gasteiger, Fuel Cell Electrocatalysis: Handbook of Fuel Cells-Fundamentals Technologies and Applications, vol. 2, Wiley, 2003.
[21] P.S. Lambrou, A.M. Efstathiou, J. Catal. 240 (2006) 182–193.
[22] M. Neergat, A.K. Shukla, K.S. Gandhi, J. Appl. Electrochem. 31 (2001) 373–378.
[23] A.S. Aricó, A.K. Shukla, H. Kim, S. Park, M. Min, V. Antonucci, Appl. Surf. Sci. 172 (2001) 33–40.

[24] W. Li, W. Zhou, H. Li, Z. Zhou, B. Zhou, G. Sun, Q. Xin, Electrochim. Acta 49 (2004) 1045–1055.
[25] N.M. Markovic, T.J. Schmidt, V. Stamenkovic, P.N. Ross, Fuel Cells 1 (2001) 105–116.
[26] D. Chu, S. Gilman, J. Electrochem. Soc. 141 (1994) 1770–1773.
[27] R. Cai, S. Song, B. Ji, W. Yang, Q. Xin, G. Sun, S. Douvartzides, P. Tsiakaras, Appl. Catal. B 61 (2005) 184–191.
[28] K. Kinoshita, Electrochemical Oxygen Technology, Wiley, New York, USA, 1992.
[29] A. Capon, R. Parsons, J. Electroanal. Chem. 44 (1973) 239–254.